Journal of Applied Polymer Science

WILEY

Applied Polymer SCIENCE

RESEARCH ARTICLE OPEN ACCESS

Reactive Oligomeric Compatibilizers: Chain Length and Additive Effects on PLA/PBAT Phase Interaction

Lena Marbach[1,2] | Viktoria Tschalabov[3] | Philip Mörbitz[1]

[1]Department for Circular and Biobased Plastics, Fraunhofer UMSICHT, Oberhausen, Germany | [2]Department of Chemistry and Biochemistry, Ruhr University, Bochum, Germany | [3]Chair of Bioinorganic Chemistry, RWTH Aachen University, Aachen, Germany

Correspondence: Lena Marbach (lena.marbach@outlook.com; lena.marbach@umsicht.fraunhofer.de)

Received: 16 April 2025 | **Revised:** 11 July 2025 | **Accepted:** 12 July 2025

Funding: The authors received no specific funding for this work.

Keywords: biopolymers and renewable polymers | compatibilization | differential scanning calorimetry (DSC) | rheology | structure-property relationships

ABSTRACT

Polylactic acid (PLA) and poly(butylene adipate-co-terephthalate) (PBAT) are promising biodegradable polymers, but their inherent immiscibility limits their use in blend applications. This study develops oligomeric compatibilizers based on PLA and PBAT, combined with epoxidized soybean oil (ESBO) and adipic acid, to enhance their compatibility. The synthesis systematically varies the molecular weight and composition of the compatibilizers. Rheological, thermal, and molecular analyses reveal that compatibilizers containing short-chain PLA and short-chain PBAT ($M_n = 3200–3800\,g\,mol^{-1}$), modified with both ESBO and adipic acid, achieve the most homogeneous phase structure. These systems exhibit single, broad T_g transitions (e.g., B1b: −3.2°C), increased viscosity (×1.8), and distinct relaxation spectra indicating strong interfacial interactions. In contrast, long-chain PBAT formulations show reduced compatibilization due to steric hindrance. IR spectroscopy confirms epoxy group reactivity; DSC reveals improved thermal transitions; and GPC/NMR validate molecular design. The results demonstrate that careful molecular design and reactive modification create effective compatibilizers, which potentially improve mechanical properties and processability in PLA/PBAT blends. These findings provide valuable insights into tailoring compatibilizer systems for sustainable biopolymer applications and lay the foundation for future investigations in commercial blend formulations.

1 | Introduction

Polylactic acid (PLA) is a biopolymer derived from renewable resources such as corn and sugarcane. Known for its biodegradability and properties comparable to conventional petrochemical plastics, PLA has found broad applications in packaging (e.g., food containers, compostable films), agriculture (e.g., mulch films), and biomedicine (e.g., sutures and drug delivery systems) [1, 2]. However, each application faces specific challenges like brittleness and poor impact resistance, which limit its use in rigid packaging. Insufficient elongation hinders its deployment in flexible films. These drawbacks include low impact strength ($< 10\,kJ/m^2$), poor elongation at break (< 10%), and brittle fracture behavior under stress [3, 4]. For packaging applications, these values fall below industrial thresholds, which typically require $\geq 30\,kJ/m^2$ impact resistance and elongation above 100%. Overcoming these drawbacks is essential to fully realize PLA as a sustainable alternative to conventional plastics [5, 6].

Blending PLA with other polymers offers a promising route to improve its performance. Poly(butylene adipate-co-terephthalate) (PBAT) complements PLA with its flexibility, toughness, and biodegradability. PLA/PBAT blends demonstrate improved ductility, impact resistance, and toughness. However, due to their differing molecular structures, PLA and PBAT are immiscible, leading to phase separation and weak interfacial adhesion. This incompatibility undermines the mechanical and structural properties of the blends, especially under demanding conditions

[7]. Effective strategies are therefore required to overcome this molecular incompatibility.

Previous strategies to address this issue include the use of block copolymers [8] reactive epoxy-functionalized additives [3] and even nanofillers as phase compatibilizers [9]. While these methods have shown partial success, they often rely on petrochemical components, lack structural flexibility, or result in inconsistent phase dispersion. In contrast, the compatibilizer approach proposed in this study enables the in situ formation of reactive oligomers with tailored chain lengths and a modular combination of functional groups.

Unlike established systems such as maleic anhydride-grafted polyesters [10] or pre-synthesized block copolymers [11], this strategy avoids permanent backbone modification and allows for a higher degree of chemical tunability. In addition, all components used, PLA, PBAT, ESBO, and adipic acid, are commercially available and partially biobased, supporting the development of sustainable, high-performance polymer blends.

Compatibilization plays a key role in improving interfacial adhesion and overall blend performance. Compatibilizers enhance mechanical, thermal, and morphological properties by fostering interactions between the PLA and PBAT phases. Compatibilizers have been shown to increase tensile strength by up to 40%, improve elongation at break from $<10\%$ to $>100\%$, and reduce phase separation, as evidenced by morphological and rheological studies [1, 12], including the use of reactive agents, block copolymers, and advanced processing methods. For example, combining epoxidized soybean oil (ESBO) with electron beam irradiation has shown promising improvements in PLA/PBAT blends [13]. It is hypothesized that irradiation promotes the formation of miscible copolyesters from oligomeric PLA and PBAT, acting as in situ compatibilizers that improve interfacial adhesion and phase continuity.

This study focuses on the development and characterization of such oligomeric compatibilizers, produced from PLA and PBAT with ESBO and adipic acid. Rheological analysis serves as a central tool to evaluate the efficiency of compatibilization. By measuring viscosity, storage modulus, and loss modulus, the study assesses phase continuity and interfacial interactions. In particular, the weighted relaxation time spectrum provides insights into the molecular dynamics and effectiveness of the compatibilizers [14].

Improved compatibilization not only enhances the mechanical performance of PLA/PBAT blends but also supports more uniform biodegradation, contributing to environmental sustainability [15]. While rheological and thermal methods offer indirect evidence of phase integration, they do not fully capture bulk mechanical behavior. Conventional mechanical testing (e.g., tensile or impact strength) would provide additional insight into the practical performance of these materials. This limitation is acknowledged in the present work and opens avenues for future investigation.

Recent work by Zhou et al. demonstrated compatibilization of PLA/PBAT blends via poly(lactic acid-r-malic acid) copolymers, achieving enhanced toughness through reactive copolymerization [4]. However, this method requires backbone modification and lacks the modular flexibility of the approach presented here.

While ESBO has previously been explored as a compatibilizer in PLA/PBAT systems, our study uniquely investigates its role in custom-designed oligomeric compatibilizers with tunable chain length and the inclusion of bifunctional additives like adipic acid. This molecular-level design enables deeper insights into phase integration and reactive dynamics, going beyond conventional compatibilizer strategies.

Furthermore, the results provide a foundation for subsequent investigations on the performance of these compatibilizers in commercial PLA/PBAT systems.

2 | Materials and Methods

2.1 | Materials

1,4-Butanediol (CP grade, $\geq 95\%$) was purchased from Carl Roth GmbH + Co. KG, Karlsruhe, Germany. L-lactide, tin(II)-2-ethylhexanoate (CP grade, $\geq 95\%$) and dimethyl terephthalate (AR grade, $\geq 99\%$) were provided by Sigma-Aldrich Chemie GmbH, Schnelldorf, Germany. Adipic acid (AR grade, $\geq 99\%$) was supplied by Fluka Chemie GmbH, Buchs, Switzerland. Terephthalic acid (AR grade, $\geq 99\%$) and titanium tetrabutanolate (CP grade, $\geq 95\%$) were acquired from Merck KGaA, Darmstadt, Germany. Merginant ESBO (technical grade, 6.5%–7.5% epoxy oxygen) was obtained from Hobum Oleochemicals, Hamburg, Germany. Ethanol (AR grade, $\geq 96\%$) and dichloromethane (AR grade, $\geq 96.5\%$) were purchased from Carl Roth GmbH + Co. KG, Karlsruhe, Germany.

2.2 | Synthesis of Oligomers and Compatibilizers

2.2.1 | Synthesis of PLA-Oligomer

L-lactide was recrystallized in ethyl acetate and dried in a high vacuum oven at 60°C for 24 h. Twenty-two equivalents of the monomer were melted at 120°C in a three-necked round bottom flask equipped with a reflux condenser and under a nitrogen atmosphere. The temperature was increased to 160°C, and 1 equivalent of the initiator 1,4-butanediol and 1.0 wt% of the catalyst tin(II)-ethylene hexanoate were added to the reaction. The reaction progress was monitored by IR spectroscopy, and the reaction was stopped when lactide consumption was complete. After cooling to room temperature, the oligomer melt was dissolved in DCM and precipitated in cold ethanol. The solid was filtered and dried in a high vacuum oven for 3 days to yield a white powder as the final product.

2.2.2 | Synthesis of PBAT-Oligomers

Polycondensation was conducted according to a procedure by Nifant'ev et al. [16]. One equivalent dimethyl terephthalate, 2.7 respective 2.4 equivalents of 1,4-butanediol, and 0.1 wt% of titanium tetrabutanolate were introduced into a three-necked round bottom flask equipped with a nitrogen inlet and a distillation bridge with receiver flask. The reaction was heated for 1 h with the removal of methanol and THF. One equivalent of adipic acid was added, and the reaction temperature was raised to 180°C. After 45 min, the nitrogen inlet was replaced with a

glass stopper, and a vacuum pump with cooling trap was connected to the distillation bridge. The pressure was gradually reduced. The reaction was terminated when the formation of water stopped. The melt was cooled to room temperature and dissolved in DCM. Cold ethanol was used for precipitation. The solids were filtered off and dried in a high vacuum drying oven for 3 days. The oligomer was yielded as a white powder.

2.2.3 | Formation of Oligomeric Compatibilizers

The 90.0 g of PLA were mixed with 90.0 g of PBAT in a 500 mL three-necked flask. Depending on the composition, 12.6 g of ESBO or 12.6 g of ESBO and 3.96 g of adipic acid were added, and the reaction was performed at 180°C for 2 h under mechanical stirring. The hot oligomer melt was poured onto a silicone mat and cooled at room temperature. In this study, a single PLA length of 3261 g mol^{-1} (referred to as S-PLA) was chosen, while two PBAT lengths of 3500 g mol^{-1} (referred to as S-PBAT) and 6500 g mol^{-1} (referred to as L-PBAT) were included. S-PLA was selected due to its lower crystallinity and enhanced chain mobility, which improve phase dispersion and interfacial compatibility with PBAT. These thermal properties, along with reduced viscosity, facilitate better processing and blending. In contrast, both S- and L-PBAT were utilized to balance flexibility, mechanical strength, and miscibility with ESBO and PLA. S-PBAT enhances compatibility with PLA, while L-PBAT contributes to greater mechanical robustness through stronger molecular networks. This combination allows for a comprehensive evaluation of phase compatibility and mechanical performance. Adipic acid was included as a bifunctional carboxylic acid that can react with hydroxyl groups present in PLA and PBAT oligomers, potentially forming ester linkages. Additionally, its small size may promote interfacial interactions and reduce phase separation by creating branched or partially crosslinked structures, which enhance compatibility between the polymer phases. The compositions of the compatibilizers are listed in Table 1.

2.3 | Analytical Methods

2.3.1 | Differential Scanning Calorimetry (DSC)

Thermal properties were analyzed using a DSC 204 F1 Phönix instrument. Using the software NETZSCH Proteus Software, values for glass transition temperature T_g, cold crystallization temperature T_{cc}, melting temperature T_m, enthalpy of cold crystallization ΔH_{cc}, enthalpy of melting ΔH_m and the change in heat capacity Δc_p were determined. For sample preparation, a quantity of 6–8 mg of the sample material was sealed in an aluminum crucible with a pierced lid. The measurement method for PLA samples starts by heating to 200°C at a rate of 20°C min^{-1} and maintaining this temperature for 10 min. The samples are then cooled to room temperature at the same rate. The second heating cycle reaches 200°C at a rate of 10°C min^{-1}, after which the samples are cooled to room temperature. PBAT samples and samples of compatibilizers follow a similar method, despite cooling to −80°C after the first heating cycle. For evaluating thermal properties only, the second heating cycle is relevant to eliminate thermal history. The crystallinity is calculated using the theoretical melting enthalpy values of a fully crystalline polymer, which are 93 J g^{-1} for PLA and 114 J g^{-1} for PBAT [17, 18].

2.3.2 | Gel Permeation Chromatography (GPC)

A GPC instrument (Agilent 1100 series, PSS GmbH, Mainz, Germany) is used to determine the molecular weights and weight distributions of oligomer samples. Polymethylmethacrylate with a low molecular weight and narrow distribution is used as a standard sample for calibration. Oligomer samples (9.0–9.5 mg) are dissolved in 1,1,1,3,3,3-hexafluoro-2-propanol (3 mL) containing potassium trifluoroacetate (0.05 mol L^{-1}). After complete dissolution, the sample is filtered through a PTFE membrane filter with a pore size of 0.45 µm. Each sample (100 µL) is injected into the mobile phase using an isocratic pump (G1310A, Agilent Series 1100) and passed through the GPC columns at a flow rate of 1 mL min^{-1}. The column set consists of three columns connected in series (PSS GmbH, Mainz, Germany). As the components exit the columns, they are detected by a refractive index (RI) detector (G1362, Agilent 1100 series). The results of the GPC measurements are analyzed by the software WinGPC UniChrom, version 8.3, PSS GmbH, Mainz, Germany, by calculating the number-average molecular weights (M_n) of the samples.

2.3.3 | Nuclear Magnetic Resonance Spectroscopy (NMR)

1H NMR spectroscopy was measured with a Bruker Ascend Evo 400 spectrometer at 400 MHz and room temperature. For this purpose, 15 mg of dried oligomer sample was dissolved in 1 mL

TABLE 1 | Compositions of the oligomeric compatibilizers.

Oligomeric compatibilizer	S-PLA [g]	S-PBAT [g]	L-PBAT [g]	ESBO[g]	Adipic acid [g]
B1	90	90			
B1a	90	90		12.6	
B1b	90	90		12.6	3.96
B2	90		90		
B2a	90		90	12.6	
B2b	90		90	12.6	3.96

$CDCl_3$ with tetramethyl silane (0.03 vol.%) stabilized with Ag. The measurement results were analyzed using the MestReNova software. Automated phase and baseline corrections were performed for each sample.

2.3.4 | Infrared Spectroscopy (IR)

A Vertex 70 (Bruker GmbH, Ettlingen, Germany) coupled with a Golden Gate ATR (Golden Gate, Specac Ltd., Orpington, UK) was employed for measurement of IR spectra. A sample is placed on the ATR crystal and affixed with a stamp. The measurements are performed with 16 scans and a resolution of 4 cm^{-1}. The measuring range includes wavelengths from 400 to 4000 cm^{-1}. Results were evaluated with the OPUS software.

2.3.5 | Rheological Investigation

Rheological measurements were performed using a MCR 302e (Anton Paar GmbH, Ostfildern, Germany) rheometer. To determine the linear viscoelastic region, an amplitude sweep test is performed. The strain amplitude is increased from 0.01% to 100% at a constant angular frequency of 100 rad s^{-1}. Subsequently, a frequency sweep is carried out within the identified linear elastic region (here, 0.1%) over a frequency range of 0.01–100 Hz. The measurements had to be performed at different temperatures due to the varying melting points of the samples. It was crucial to ensure the presence of a homogeneous melt that was sufficiently fluid to allow reliable measurements, but not excessively fluid to avoid distortions in the rheological behavior. This suitable temperature range is particularly narrow for oligomeric materials, requiring careful optimization to capture representative flow properties under comparable conditions. The chosen temperature was 140°C for PLA oligomers, 120°C for PBAT, and 130°C for the oligomeric compatibilizers. Complex viscosity (η^*), storage modulus (G'), and loss modulus (G'') are determined. Subsequently, the weighted relaxation time spectrum $H(\lambda)\lambda$, which characterizes the distribution of relaxation times in the material, is calculated. The relaxation times λ themselves can be extracted from the characteristic frequencies at which the material exhibits significant spectral contributions to its viscoelastic response. The software RheoCompass was used for evaluation.

3 | Results and Discussion

Characterization of a total of six oligomeric compatibilizers was performed. The compatibilizers consist of a combination of S-PLA ($M_n = 3261$ g mol^{-1}) with either S- or L-PBAT ($M_n = 3500$ and 6500 g mol^{-1}). Compatibilizers were prepared without additives, with ESBO, or with ESBO and adipic acid as additives.

3.1 | Molecular Mass Determination Using GPC and NMR

Molecular masses of the oligomers are determined by both gel permeation chromatography and nuclear magnetic resonance spectroscopy. The results are listed in Table 2.

TABLE 2 | Target molecular masses and masses determined by GPC and NMR.

Oligomer	$M_{n,target}$ [g mol^{-1}]	$M_{n,GPC}$ [g mol^{-1}]	$M_{n,NMR}$ [g mol^{-1}]
S-PLA	3261	6680	4144
S-PBAT	3500	3790	3255
L-PBAT	6500	7950	5702

Note: GPC values refer to PMMA standards; NMR values are absolute molecular weights based on end-group analysis.

The experimentally determined molecular weights of PLA exceeded the targeted values, a discrepancy that can be attributed to product purification via precipitation. During this process, lower molecular weight chains, which contribute to the lower end of the molecular weight distribution, were selectively removed. Consequently, the number-average molecular weight (M_n) exhibited an upward shift. For PLA, a molecular weight of 6680 g mol^{-1} was obtained through gel permeation chromatography. The oligomeric structure of PLA was subsequently analyzed by proton nuclear magnetic resonance spectroscopy. The integral values of the signals corresponded to the number of protons present. Based on this analysis, the molecular weight was determined to be 4144 g mol^{-1}. The differences between the molar masses determined by GPC and NMR are probably caused by the different preparation methods for the measurements. Additionally, GPC results are relative to a PMMA standard, while NMR results are absolute values.

The chemical composition of S-PBAT was investigated using ^{1}H NMR. The ratio between the dimethyl terephthalate and adipic acid units was found to be 1:1, aligning with the intended target ratio. Analysis of the chain-end signals indicated that 20% of oligomer chains terminated with a methyl group, while 80% of oligomer chains terminated with a hydroxyl group from 1,4-butanediol. The molecular weight, calculated from ^{1}H NMR data, was 3255 g mol^{-1}, closely matching the expected value.

Similarly, the ^{1}H NMR spectrum of L-PBAT confirmed that the ratio between the dimethyl terephthalate and adipic acid units was maintained at 1:1, as intended. The chain-end group analysis revealed that 46% of oligomer chains terminated with methyl groups, while 54% terminated with hydroxyl groups. The molecular weight, determined via ^{1}H NMR, was calculated to be 5702 g mol^{-1}, which closely approximated the target molecular weight. All ^{1}H NMR spectra are presented in Figures S1–S3. GPC measurements for S-PBAT yielded a number-average molecular weight of 3790 g mol^{-1}, while for L-PBAT, the measured M_n was 7950 g mol^{-1}. GPC retention curves are presented in Figures S4 and S5.

3.2 | Infrared Spectroscopy

Infrared spectroscopy is used to investigate the presence and reactivity of epoxy groups in the oligomeric compatibilizers. The characteristic absorption band of the epoxy groups in ESBO appears at 823 cm^{-1}. Figure 1 presents the magnified spectra in this region for the different compatibilizer compositions. The full spectra are shown in Figures S6 and S7.

Among all samples, only B2b shows a visible increase in absorbance at 823 cm^{-1}. This indicates that in B2b, some epoxy groups remain unreacted, while in the other samples, the epoxy functionalities have likely reacted completely. The presence of unreacted epoxy groups in B2b could result from sample inhomogeneity, where measured particles contain locally high concentrations of ESBO, or from a slower reaction rate of longer PBAT chains. Based on the IR absorption behavior and chain-end analysis, it is likely that PLA, with its higher proportion of hydroxyl end groups, reacts more readily with ESBO's epoxy moieties. PBAT oligomers, particularly the longer chains, showed reduced reactivity, possibly due to steric hindrance or lower end-group concentration. This suggests a preferential reaction of ESBO with PLA, forming PLA-rich graft or crosslinked domains. Furthermore, it is important to consider that ESBO contains a relatively low number of epoxy groups, and the dilution effect in the oligomer blend generally weakens the intensity of the corresponding IR bands.

3.3 | Differential Scanning Calorimetry

Thermal properties of the oligomers were obtained by DSC. The results are listed in Table 3 and the thermograms are presented in Figure 2.

Multiple overlapping melting peaks for the oligomeric structures indicate the presence of different crystalline forms, each melting at distinct temperatures [19]. This can result from heterogeneous segmental compositions with differences in crystallization kinetics. A potential explanation for PLA's low crystallinity in this case is the high concentration of 1,4-butanediol. This compound interferes with the crystallization process by disrupting the orderly packing of polymer chains, reducing the overall degree of crystallinity. In the case of PBAT, the glass transition temperature of S-PBAT is slightly lower than that of L-PBAT. Since T_g is closely linked to chain mobility, this observation suggests that S-PBAT oligomers exhibit greater molecular flexibility, likely due to reduced entanglement and a lower degree of intermolecular interactions. Shorter chains offer fewer interaction points, which facilitates faster segmental motion and thus leads to a lower T_g [20].

Interestingly, despite its lower molecular weight, S-PBAT exhibits a slightly higher melting temperature compared to L-PBAT. This apparent contradiction can be explained by the fact that shorter chains are able to pack more efficiently into regular lamellar structures, resulting in higher crystalline perfection and more stable crystallites. In contrast, the longer chains of L-PBAT may adopt more coiled or irregular conformations, hindering dense packing and lowering the thermal stability of the crystalline domains.

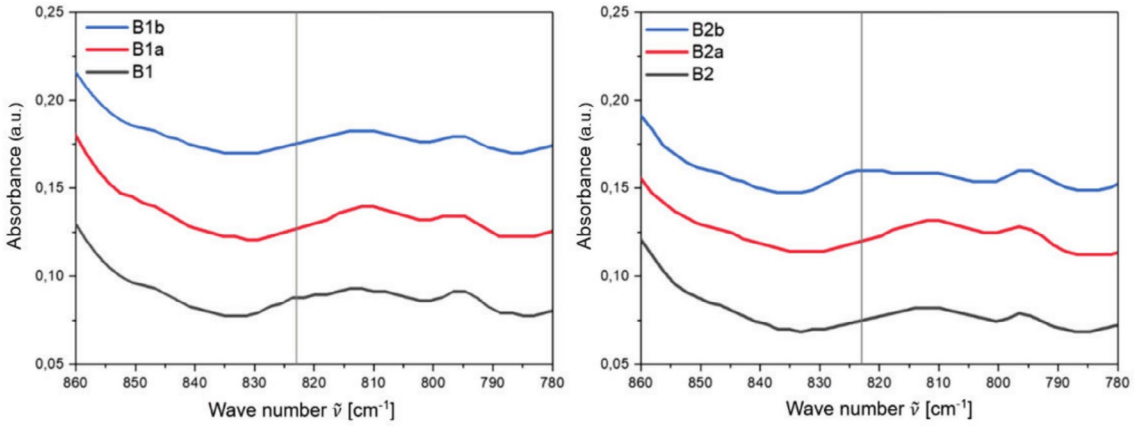

FIGURE 1 | Magnified spectra in the range of 860–780 cm^{-1} of the oligomeric compatibilizers. [Color figure can be viewed at wileyonlinelibrary.com]

TABLE 3 | Thermal properties of PLA and PBAT oligomers.

Sample	Δc_p [$J g^{-1} K^{-1}$]	T_g [°C]	T_{cc} [°C]	T_m [°C]	ΔH_{cc} [$J g^{-1}$]	ΔH_m [$J g^{-1}$]	X_c [%]
S-PLA	0.576	37.8	101.9	120.2	−25.7	29.10	3.66
				130.7			
				139.2			
S-PBAT	0.094	−38.3	—	128.2	—	9.41	8.25
				140.8			
L-PBAT	0.232	−37.8	—	117.1	—	17.35	15.22
				132.2			

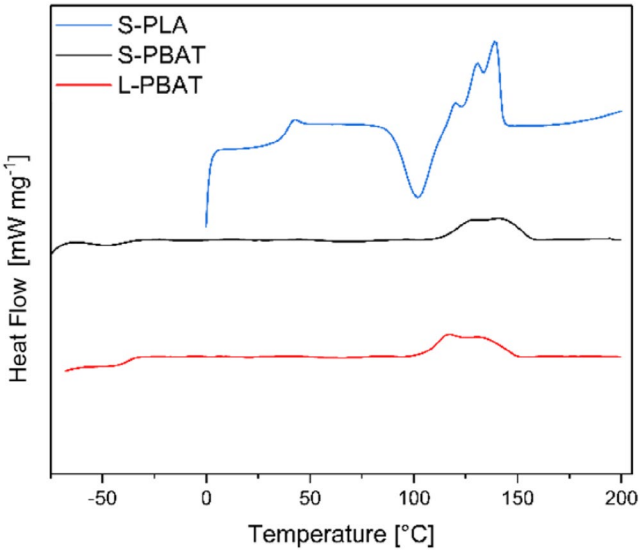

FIGURE 2 | Thermograms of the oligomers S-PLA, S-PBAT and L-PBAT. [Color figure can be viewed at wileyonlinelibrary.com]

However, L-PBAT shows nearly twice the degree of crystallinity compared to S-PBAT. This is likely because longer chains provide more segmental length to participate in crystalline regions, leading to an overall increase in the quantity of crystalline domains, even if they are less perfect. The combination of these thermal parameters highlights that crystallinity, melting temperature, and glass transition temperature are influenced by both chain length and chain packing behavior, and cannot be interpreted solely based on molecular weight.

The measurement values for DSC of the oligomeric compatibilizers are listed in Table 4 and the thermograms are presented in Figure 3. Crystallinity is not calculated, as overlapping enthalpy contributions from PLA cold crystallization and PBAT melting complicate accurate determination.

Polymers, respectively oligomers, with complete miscibility typically show only one T_g. Insufficient miscibility will show two T_g's corresponding to the initial oligomers [21]. Almost all compatibilizers in this series have two T_g, indicating that they have insufficient miscibility. The exceptions are samples B1b

TABLE 4 | DSC results of oligomeric compatibilizers B1–B2.

Sample	PLA	PBAT	Δc_p [J g^{-1} K^{-1}]	T_g [°C]	T_{cc} [°C]	T_m [°C]	ΔH_m [J g^{-1}]
B1	S-PLA	S-PBAT	0.147	−21.4	69.4	125.0	21.13
			0.094	15.7			
B1a	S-PLA	S-PBAT	0.074	−27.3	72.7	131.2	25.77
			0.219	30.7			
B1b	S-PLA	S-PBAT	0.328	−3.2	71.5	122.7	18.78
B2	S-PLA	L-PBAT	0.129	−23.7	77.6	109.2	19.73
			0.213	22.5		125.7	
B2a	S-PLA	L-PBAT	0.164	−29.0	78.8	113.2	28.42
			0.424	34.7		131.5	
B2b	S-PLA	L-PBAT	0.112	−17.5	72.6	106.2	19.63
						123.5	

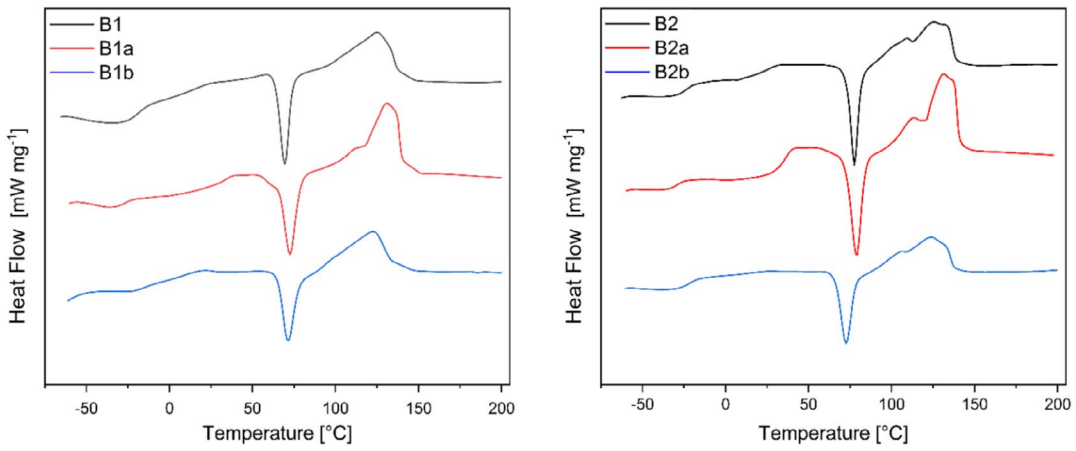

FIGURE 3 | Thermograms of the oligomeric compatibilizers B1 (left) and B2 (right). [Color figure can be viewed at wileyonlinelibrary.com]

and B2b, which show a glass transition temperature at −3.2°C and −17.5°C respectively, with a broad transition, especially for B1b. In the case of B1b, the single, broad glass transition temperature lies approximately midway between the values for pure PLA and PBAT oligomers. This suggests that the combination of short chain PLA and short chain PBAT promotes efficient reactive compatibilization with ESBO and adipic acid. The higher chain mobility of S-PBAT likely facilitates better integration and reaction with the PLA and reactive additives, leading to a more homogeneous phase and improved molecular-level mixing [7]. In contrast, B2b exhibits a single glass transition temperature shifted closer to that of PBAT. The infrared spectroscopy results show that this sample retains unreacted epoxy groups, indicating incomplete reaction of ESBO with the polymer chains. The higher molecular weight of L-PBAT likely limits the reactivity due to steric hindrance and reduced mobility, which restricts the formation of a fully integrated compatibilizer network. As a result, the PBAT phase dominates the thermal behavior, reflected by a T_g closer to PBAT.

Samples B1a and B2a show a divergence of the T_g in comparison to samples B1 and B2. This behavior reflects the dual role of ESBO as both a plasticizer and a reactive additive. In the PBAT phase, ESBO acts predominantly as a plasticizer, increasing chain mobility and free volume, which lowers the T_g. However, in the PLA phase, ESBO may react with hydroxyl or carboxyl end groups of the PLA oligomers, leading to restricted chain mobility through branching or limited crosslinking. This reaction effectively counteracts the plasticizing effect and results in an increase of the PLA-related T_g. These observations suggest that the impact of ESBO on thermal transitions depends strongly on its interaction with the respective polymer phases, highlighting the complex balance between physical plasticization and chemical reactivity in the system [22].

The cold crystallization temperature is lower in compatibilizers containing S-PBAT, suggesting that shorter PBAT chains improve mobility and integration into the PLA matrix. Higher chain mobility allows better distribution of PBAT within the PLA phase, enhancing interactions between the polymers. As a result, fewer free PLA chains are available to reorganize and crystallize, which shifts the recrystallization process to lower temperatures. These observations strengthen the overall conclusion that the molecular weight and chain mobility of PBAT play a significant role in influencing thermal transitions and blend morphology.

3.4 | Rheological Analysis

3.4.1 | Complex Viscosity

The mechanical behavior of oligomers, particularly their viscoelastic properties, can be comprehensively understood by examining their complex viscosity (η^*), storage modulus (G'), and loss modulus (G'') in relation to chain interactions and molecular weight. For the unmodified oligomers, the complex viscosity of L-PBAT is the lowest, followed by S-PLA, with S-PBAT exhibiting the highest viscosity. This trend is consistent with the molecule structures, as PLA is a stiff and rigid oligomer. Its methyl side groups facilitate intermolecular interactions, enhancing its resistance to flow. L-PBAT, which has a lower glass transition temperature than PLA, demonstrates lower viscosity due to its highly flexible aliphatic backbone, despite being measured at a lower temperature. S-PBAT exhibits the highest viscosity due to its higher melting temperature, listed in Table 4, resulting in hindered movement. The shorter PBAT chains are capable of packing more efficiently and undergo more intermolecular interactions, which lead to a higher melting temperature, resulting in a higher viscosity as L-PBAT. The complex viscosities are depicted in Figure 4.

Subsequently, the viscosities of oligomeric compatibilizers B1–B2 are analyzed and shown in Figure 5. B1 and B2 exhibit nearly identical viscosities, indicating that the sole factor of the components chain length does not have an influence on the viscosity. A substantial increase in viscosity is observed in B1a, suggesting that ESBO promotes interactions between PLA and PBAT phases. This is consistent with the thermal analysis, where B1a displays the highest melting temperature among the B1 compatibilizers, indicating improved phase integration. B2a has the lowest viscosity, possibly due to the reduced miscibility of PLA and PBAT, attributed to the higher PBAT molecular mass, making ESBO more likely to function as a plasticizer in PBAT phases, aligning with the observations made on the thermal properties. Additionally, ESBO is more soluble in PBAT due to PBAT's aliphatic segments. When PBAT has a lower molecular mass, it is more likely to be well-distributed within PLA, with ESBO also being homogeneously distributed. The introduction of adipic acid lowers the viscosity for B1b and increases it for B2b, indicating that the length of PBAT oligomers influences the distribution and interaction of ESBO and adipic acid. These opposing effects of adipic acid can be attributed to differences in PBAT chain length and their resulting interaction dynamics within the compatibilizer matrix. In B1b, which contains short-chain PBAT, adipic acid may act as a chain-terminating agent or promote limited branching through esterification reactions. Due to the shorter backbone, the probability of intramolecular reactions or chain scission is higher, resulting in reduced molecular entanglement and lower complex viscosity.

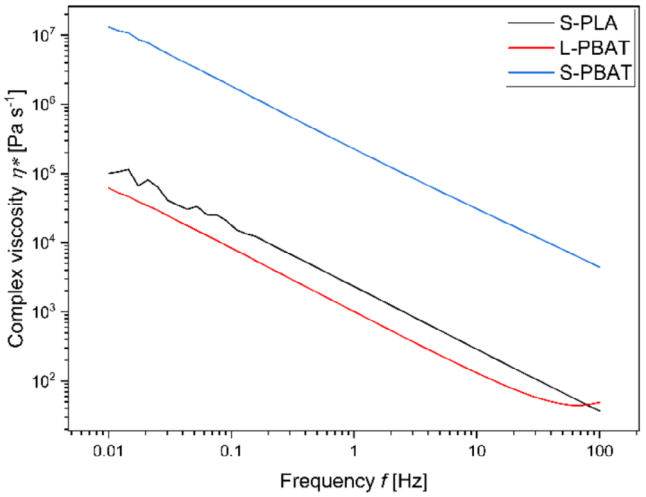

FIGURE 4 | Complex viscosities of the oligomers S-PLA, S-PBAT, and L-PBAT. [Color figure can be viewed at wileyonlinelibrary.com]

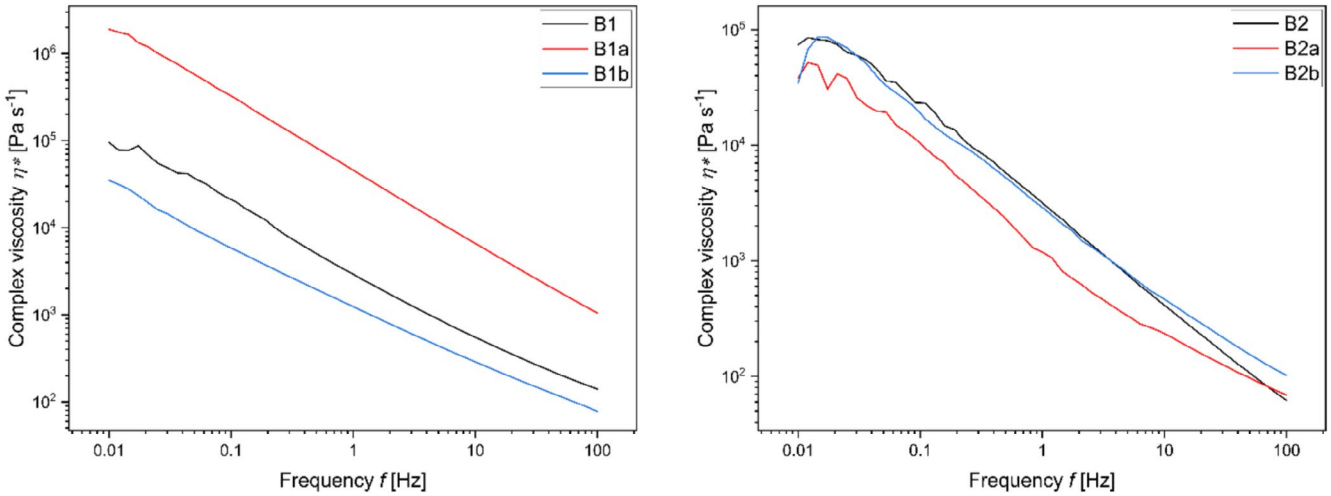

FIGURE 5 | Complex viscosities of the oligomeric compatibilizers B1 (left) and B2 (right). [Color figure can be viewed at wileyonlinelibrary.com]

In contrast, in B2b, which includes long-chain PBAT, the presence of more extended polymer backbones provides increased accessibility and spatial separation between functional groups. This spatial arrangement favors intermolecular over intramolecular reactions, enabling adipic acid to act as a bifunctional crosslinker. This results in a denser molecular architecture, enhanced chain coupling, and a corresponding increase in complex viscosity. The increase in modulus observed in rheological analysis supports this interpretation.

3.4.2 | Loss- and Storage Modulus

Analyzing the storage modulus (G') and loss modulus (G'') gives insights about viscoelastic properties. The results are depicted in Figure 6. Among the unmodified oligomers, S-PBAT exhibits the highest values for both G' and G'' across the entire frequency range, which reflects its higher melting temperature and the resulting restricted chain mobility. In contrast, L-PBAT shows the lowest moduli, indicating a softer, more flexible character due to its longer chains and higher chain mobility. S-PLA falls between these two extremes, with a storage modulus higher than that of L-PBAT but significantly lower than S-PBAT.

The frequency-dependent trends reveal that at low frequencies, all materials exhibit lower G' and G'' values, characteristic of fluid-like behavior. As the frequency increases, both moduli rise, indicating a transition toward a more solid-like response. This effect is especially pronounced in L-PBAT, where G' increases noticeably at higher frequencies, suggesting that the material develops structural stiffness under rapid deformation, likely due to temporary chain entanglements.

From a viscoelastic perspective, G' represents the ability of a material to store mechanical energy, while G'' accounts for energy dissipation. When G' exceeds G'', the material behaves more elastically, whereas a dominant G'' suggests a more viscous character. The results indicate that all samples exhibit elastic behavior, with the storage modulus being greater than the loss modulus. In conclusion, S-PBAT is the stiffest and most

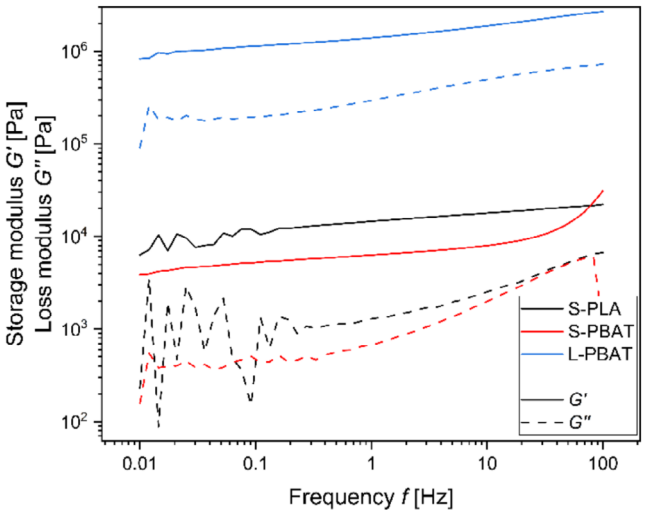

FIGURE 6 | Storage modulus (G') and loss modulus (G'') of the oligomers S-PLA, S-PBAT and L-PBAT. [Color figure can be viewed at wileyonlinelibrary.com]

structurally stable material, followed by S-PLA, which has moderate rigidity, and L-PBAT, which is the softest and most flexible.

The storage and loss moduli of the compatibilizers are presented in Figure 7. For the oligomeric compatibilizers composed of S-PLA and S-PBAT, sample B1a exhibits the highest G' and G'' values across all frequencies, indicating that the addition of ESBO enhances stiffness and elasticity. This finding aligns with the previously observed increase in viscosity and melting temperature, suggesting stronger interactions and improved phase integration. B1, without additives, shows intermediate mechanical properties, representing a balance between elasticity and viscosity. In contrast, B1b demonstrates the lowest moduli, implying that the addition of adipic acid softens the material, likely by chain scission reactions resulting in increased chain mobility. At lower frequencies, all B1 series samples exhibit fluid-like behavior, while at higher frequencies, their moduli rise, with B1a maintaining the highest values and B1b remaining the softest. Notably, B1b displays a loss modulus higher than the storage

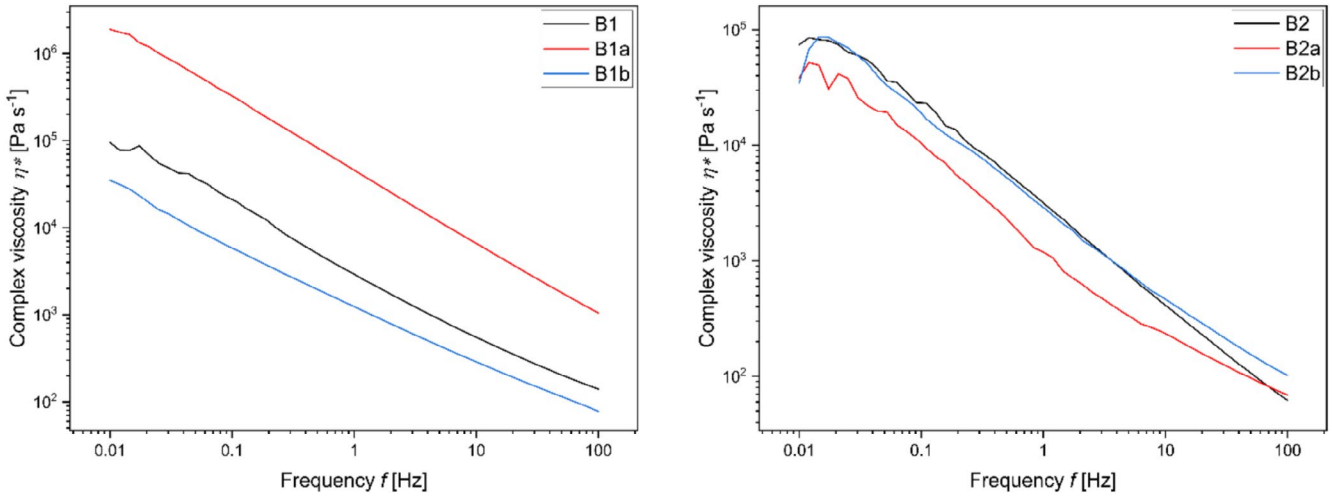

FIGURE 7 | Storage modulus (G') and loss modulus (G'') of the oligomeric compatibilizers B1 (left) and B2 (right). [Color figure can be viewed at wileyonlinelibrary.com]

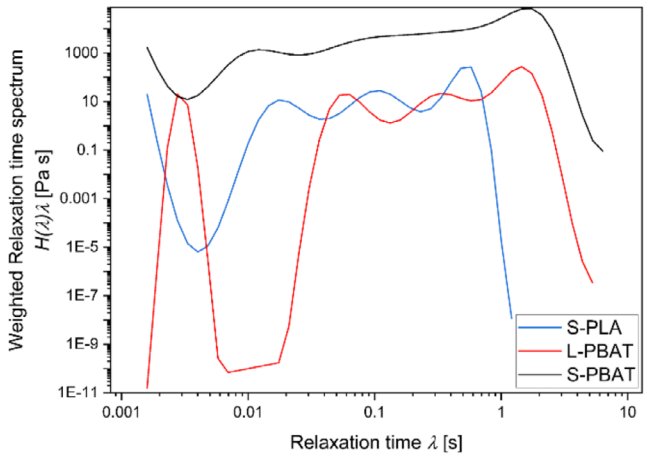

FIGURE 8 | Weighted relaxation time spectra of the oligomers S-PLA, S-PBAT, and L-PBAT. [Color figure can be viewed at wileyonlinelibrary.com]

modulus, indicating that the material behaves more like a viscous fluid due to the influence of adipic acid.

For oligomeric compatibilizers composed of S-PLA and L-PBAT all moduli show similar values with B2a showing the lowest. This could be caused by good miscibility of ESBO with the longer PBAT-chains, causing better chain mobility. The addition of adipic acid in B2b leads to a recovery in storage and loss moduli. The influence of the addition of ESBO and adipic acid shows great differences in the compatibilizers B1 and B2, suggesting that the molecular weight of PBAT has a significant influence on the moduli, in contrast to the viscosity.

3.4.3 | Relaxation Time Spectra

The weighted relaxation time spectra, shown in Figures 8 and 9, provide deeper insight into the molecular dynamics and viscoelastic behavior of the oligomeric compatibilizers. The relaxation time λ describes how quickly a material responds to deformation and returns to its equilibrium state. Generally, shorter relaxation times indicate higher chain mobility and lower viscosity, while longer relaxation times are associated with stronger intermolecular interactions and a more rigid molecular structure. The height of the peaks $H(\lambda)\lambda$ is correlated with the amount of relaxation processes. Thimm et al. investigated the connection between molecular weight and distribution on the relaxation spectrum [23]. Gramespacher et al. described how the interface between blend components can be characterized using the relaxation times [14].

The neat oligomers each exhibit multiple relaxation times, with each time scale corresponding to a distinct relaxation process. S-PLA displays short relaxation times, with a maximum of 0.578 s, indicating a brittle material that relaxes quickly after deformation. The relatively low peak height of 263.27 Pa s suggests that only a limited number of relaxation processes occur within the material.

L-PBAT shows longer relaxation times, with a maximum of 1.452 s, and a similarly low peak height of 274.16 Pa s. Notably, its relaxation times are widely distributed, ranging from as short as 0.003 s to the longer maximum values. This broad distribution indicates the presence of multiple relaxation processes over different time scales. However, as with S-PLA, the relatively low peak height implies that the number of molecules actively contributing to relaxation remains limited.

In contrast, S-PBAT exhibits the longest relaxation time at 1.746 s and an exceptionally high peak value for $H(\lambda)\lambda$, reaching 66,358.15 Pa s. This pronounced peak suggests that a significant number of molecular relaxation processes occur within the material. The extended relaxation time and high peak height indicate that S-PBAT behaves as a highly flexible oligomer, which is consistent with its structural characteristics and strong intermolecular interactions.

All B1 samples display the characteristic relaxation peak of S-PBAT at approximately 1.746 s, indicating that the structural elements of S-PBAT continue to contribute to relaxation behavior within the blend. In sample B1, the height of this peak is relatively low at 2454.76 Pa s, suggesting that many of the potential

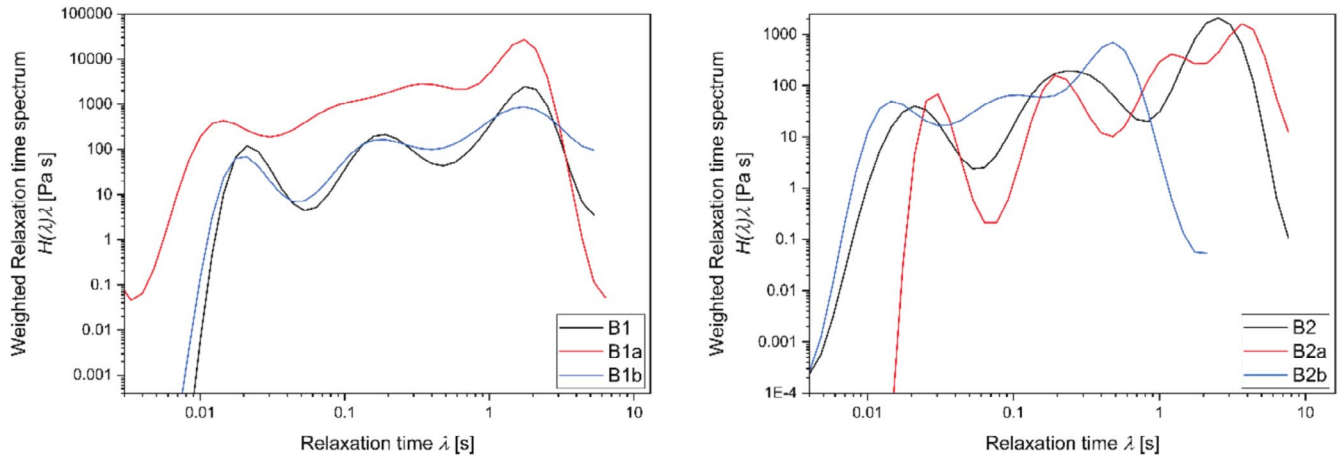

FIGURE 9 | Weighted relaxation time spectra of the oligomeric compatibilizers B1 (left) and B2 (right). [Color figure can be viewed at wileyonlinelibrary.com]

relaxation processes are restricted by the presence of PLA, which limits molecular mobility.

Upon the addition of ESBO in sample B1a, the peak height increases substantially to 27,166.35 Pa s. This significant rise supports the findings from the thermal and viscosity analyses, indicating that ESBO, being enriched in the PBAT phase, enhances chain mobility and facilitates molecular relaxation. Interestingly, B1a also exhibits relaxation times that fall between the characteristic values of S-PLA and S-PBAT. This behavior suggests that ESBO may promote chemical interactions between PLA and PBAT chains, resulting in coupled relaxation processes involving both phases. Similar findings were made by Al-Itry et al. on a PLA/PBAT blend compatibilized with a commercial oligomer [12].

In contrast, sample B1b shows an even lower peak height than B1, indicating a further suppression of molecular relaxation. This observation strongly suggests that the addition of adipic acid leads to the formation of network structures or constraints that hinder chain mobility, thereby reducing the number of effective relaxation processes within the material.

Samples B2 and B2a both exhibit relaxation times longer than those observed in the individual neat oligomers, at 2.524 s and 3.648 s, respectively. These extended relaxation times likely correspond to interphase relaxation processes, where oligomer chains located at the interface between PLA and PBAT phases become entangled. This effect is particularly enhanced by the longer chains of L-PBAT, which promote physical entanglement and limit chain mobility, thereby extending relaxation times. Similar observations have been reported by Jang et al. [24].

The addition of ESBO in sample B2a amplifies this effect, most likely by increasing the mobility of PBAT chains, which allows them to penetrate more effectively into the PLA-rich phase. Notably, B2a also displays a distinct relaxation peak at approximately 1.208 s, corresponding to the characteristic relaxation time of L-PBAT. This suggests that, despite interfacial entanglement, L-PBAT retains some degree of mobility in the presence of ESBO, supporting the role of ESBO as a partial plasticizer in this system.

When adipic acid is introduced in sample B2b, the long relaxation times disappear entirely, and only short relaxation processes remain. The shortest relaxation time, at 0.015 s, can be attributed to S-PLA, while the other two peaks at 0.092 and 0.481 s likely represent combined relaxation processes involving both PLA and PBAT chains. This pattern suggests that partial compatibilization between PLA and PBAT has occurred, resulting in a more homogeneous phase structure. Furthermore, the overall lower peak heights in B2b indicate a reduced number of relaxing molecular units, consistent with the formation of a denser and more constrained network structure. This observation suggests enhanced interfacial interactions, where chain coupling promotes a more homogeneous phase distribution, as similarly reported by Jang et al. [24]. A complete summary of the relaxation times and corresponding peak heights is provided in Table S8.

3.5 | Proposed Mechanism of Compatibilization

The observed changes in viscosity, glass transition behavior, and relaxation spectra suggest that chemical reactions take place between the components of the oligomeric compatibilizer system. A plausible mechanism involves three main pathways: epoxide ring-opening, esterification, and transesterification.

Epoxide ring-opening occurs between the epoxide groups of ESBO and terminal functional groups of the oligomeric PLA and PBAT chains. Both hydroxyl (–OH) and carboxyl (–COOH) end groups can react with the strained epoxide rings. The nucleophilic attack by a hydroxyl group forms a β-hydroxyether, whereas a carboxylic acid yields a β-hydroxyester:

$$R - OH + R' - CH(O) - CH_2 \rightarrow R - O - CH_2 - CH(OH) - R' \quad (1)$$

$$R - COOH + R' - CH(O) - CH_2 \rightarrow R - COO - CH_2 - CH(OH) - R' \quad (2)$$

These reactions result in covalent links between PLA/PBAT chains and ESBO, promoting interfacial adhesion and reducing phase separation. The abundance of reactive oxirane groups in ESBO facilitates multiple coupling points across polymer domains.

Esterification between hydroxyl and carboxylic acid end groups of PLA and PBAT oligomers further contributes to molecular linkage. This reaction occurs under melt processing conditions and results in conventional ester bonds:

$$R - COOH + R' - OH \rightleftharpoons R - COO - R' + H_2O \quad (3)$$

Lastly, transesterification may occur as a side reaction at elevated temperatures. This process exchanges ester groups between oligomers, enabling additional redistribution and coupling between chains:

$$R - COO - R' + R'' - OH \rightleftharpoons R - COO - R'' + R' - OH \quad (4)$$

Taken together, these reactions are believed to contribute to the formation of interfacial networks or block-like copolymers in situ, effectively compatibilizing the immiscible PLA and PBAT phases. The presence of adipic acid, a bifunctional diacid, may further increase network density through multiple esterification points, although direct quantification of crosslinking was not performed in this study. The observed rheological signatures (e.g., increased complex viscosity and broadened relaxation time) provide indirect evidence for these coupling reactions.

4 | Conclusions

This study demonstrates how the molecular architecture of PBAT and the selection of reactive additives critically influence the performance of oligomeric compatibilizers for PLA/PBAT blends. Short-chain PBAT enables stronger interactions with PLA, particularly in the presence of ESBO, leading to enhanced miscibility and improved mechanical properties. In contrast, long-chain PBAT exhibits limited reactivity, with ESBO primarily acting as a plasticizer unless supported by additional reactive components such as adipic acid. The combination of spectroscopic, thermal, and rheological analyses consistently confirms that both PBAT chain length and additive composition govern the balance between chain mobility, network formation, and interfacial interactions within the compatibilizer systems. While this study primarily relies on rheological and thermal indicators of phase interaction, the observed changes in viscosity and relaxation behavior suggest the possible formation of branched or weakly crosslinked structures. Although a direct quantification of crosslinking density (e.g., via gel content or rheo-NMR) was not conducted, these effects warrant further investigation in future work.

Quantitatively, sample B1a (S-PBAT + ESBO) showed a +1.8-fold increase in complex viscosity and a 3.4-fold increase in relaxation peak height compared to unmodified blends, indicating significantly enhanced interfacial interactions. Similarly, B2b (L-PBAT + ESBO + adipic acid) exhibited a unique single T_g and relaxation time compression, reflecting improved miscibility. These performance metrics are on par with or exceed those reported for compatibilizers based on epoxy-POSS [3] and block copolymers [11].

These insights lay a solid foundation for the development of tailored compatibilizer systems for biodegradable polymer blends. Future work will focus on transferring these optimized compatibilizers into commercial-grade PLA/PBAT blends to evaluate their effectiveness under application-relevant conditions. This next step aims to validate the laboratory findings at the practical scale, assess mechanical performance and processability, and contribute to the broader goal of advancing sustainable, high-performance biopolymer materials. To fully validate the compatibilization performance in practical applications, future work will also include scanning electron microscopy to assess blend morphology and tensile or impact testing to evaluate mechanical properties. These methods will allow correlation of interfacial structure with bulk behavior, particularly in commercial-grade PLA/PBAT blends.

Author Contributions

Lena Marbach: conceptualization (lead), data curation (equal), formal analysis (equal), investigation (equal), methodology (lead), visualization (equal), writing – original draft (lead), writing – review and editing (lead). **Philip Mörbitz:** conceptualization (supporting), methodology (supporting), supervision (lead), writing – review and editing (supporting). **Viktoria Tschalabov:** data curation (equal), formal analysis (equal), investigation (equal), visualization (equal), writing – original draft (equal).

Acknowledgments

The authors gratefully acknowledge the technical support provided by the Polymer Laboratory at Fraunhofer UMSICHT. Special thanks are extended to Uwe Kleinwegen and Christian Brzoska for assistance with thermal measurements. The authors also thank Hobum Oleochemicals GmbH for providing some of the material that was used in this work. Open Access funding enabled and organized by Projekt DEAL.

Conflicts of Interest

The authors declare no conflicts of interest.

Data Availability Statement

The data that support the findings of this study are available from the corresponding author upon reasonable request.

References

1. R. Muthuraj, M. Misra, and A. K. Mohanty, "Biodegradable Compatibilized Polymer Blends for Packaging Applications: A Literature Review," *Journal of Applied Polymer Science* 135, no. 24 (2018): 45726, https://doi.org/10.1002/app.45726.

2. N.-A. A. B. Taib, M. R. Rahman, D. Huda, et al., "A Review on Poly Lactic Acid (PLA) as a Biodegradable Polymer," *Polymer Bulletin* 80, no. 2 (2023): 1179–1213, https://doi.org/10.1007/s00289-022-04160-y.

3. N. T. Kilic, B. N. Can, M. Kodal, and G. Ozkoc, "Compatibilization of PLA/PBAT Blends by Using Epoxy-POSS," *Journal of Applied Polymer Science* 136, no. 12 (2019): 47217, https://doi.org/10.1002/app.47217.

4. S. Zhou, H. Yu, Y. Li, C. Qi, and J. Li, "Preparation and Characterization of PLA/PBAT Blends Toughened by Poly(Lactic Acid-r-Malic Acid)

Copolymer," *Colloid & Polymer Science* 302, no. 8 (2024): 1201–1207, https://doi.org/10.1007/s00396-024-05252-z.

5. H. Tsuji, "Poly(Lactic Acid)," in *Bio-Based Plastics: Materials and Applications*, ed. S. Kabasci (Wiley, 2014), 171–239.

6. S. Su, R. Kopitzky, and C. Berrenrath, "Experimental Determination of Molecular Weight-Dependent Miscibility of PBAT/PLA Blends," *Polymers* 13, no. 21 (2021): 3686, https://doi.org/10.3390/polym13213686.

7. S. Su, "Prediction of the Miscibility of PBAT/PLA Blends," *Polymers* 13, no. 14 (2021): 2339, https://doi.org/10.3390/polym13142339.

8. L. G. Santos, L. C. Costa, and L. A. Pessan, "Development of Biodegradable PLA/PBT Nanoblends," *Journal of Applied Polymer Science* 135, no. 12 (2018): 45951, https://doi.org/10.1002/app.45951.

9. D. Vrsaljko, D. Macut, and V. Kovačević, "Potential Role of Nanofillers as Compatibilizers in Immiscible PLA/LDPE Blends," *Journal of Applied Polymer Science* 132, no. 6 (2015): 41414.

10. A. Teamsinsungvon, Y. Ruksakulpiwat, and K. Jarukumjorn, "Poly(Lactic Acid)/poly(Butylene Adipate-Co-Terephthalate) Blend and Its Composite: Effect of Maleic Anhydride Grafted Poly(Lactic Acid) as a Compatibilizer," *Advanced Materials Research* 410 (2011): 51–54, https://doi.org/10.4028/www.scientific.net/AMR.410.51.

11. Y. Ding, B. Lu, P. Wang, G. Wang, and J. Ji, "PLA-PBAT-PLA Tri-Block Copolymers: Effective Compatibilizers for Promotion of the Mechanical and Rheological Properties of PLA/PBAT Blends," *Polymer Degradation and Stability* 147 (2018): 41–48, https://doi.org/10.1016/j.polymdegradstab.2017.11.012.

12. R. Al-Itry, K. Lamnawar, and A. Maazouz, "Rheological, Morphological, and Interfacial Properties of Compatibilized PLA/PBAT Blends," *Rheologica Acta* 53, no. 7 (2014): 501–517, https://doi.org/10.1007/s00397-014-0774-2.

13. L. Marbach and P. Mörbitz, "Electron Beam-Induced Compatibilization of PLA/PBAT Blends in Presence of Epoxidized Soybean Oil," *Polymers* 15, no. 15 (2023): 3265, https://doi.org/10.3390/polym15153265.

14. H. Gramespacher and J. Meissner, "Interfacial Tension Between Polymer Melts Measured by Shear Oscillations of Their Blends," *Journal of Rheology* 36, no. 6 (1992): 1127–1141, https://doi.org/10.1122/1.550304.

15. E. Xanthopoulou, N. Pardalis, A. Zamboulis, and D. N. Bikiaris, "Exploring the Effect of Hemp Fibers' Addition on the Properties of PLA/PPAd Biodegradable Blends," *Sustainable Chemistry for the Environment* 8 (2024): 100176, https://doi.org/10.1016/j.scenv.2024.100176.

16. I. E. Nifant'ev, V. V. Bagrov, P. D. Komarov, S. O. Ilyin, and P. V. Ivchenko, "The Use of Branching Agents in the Synthesis of PBAT," *Polymers* 14, no. 9 (2022): 1720, https://doi.org/10.3390/polym14091720.

17. H. Simmons, P. Tiwary, J. E. Colwell, and M. Kontopoulou, "Improvements in the Crystallinity and Mechanical Properties of PLA by Nucleation and Annealing," *Polymer Degradation and Stability* 166 (2019): 248–257, https://doi.org/10.1016/j.polymdegradstab.2019.06.001.

18. L. C. Lins, S. Livi, J. Duchet-Rumeau, and J.-F. Gérard, "Phosphonium Ionic Liquids as New Compatibilizing Agents of Biopolymer Blends Composed of Poly(Butylene-Adipate-Co-Terephtalate)/poly(-Lactic Acid) (PBAT/PLA)," *RSC Advances* 5, no. 73 (2015): 59082–59092, https://doi.org/10.1039/C5RA10241C.

19. S. Saeidlou, M. A. Huneault, H. Li, and C. B. Park, "Poly(Lactic Acid) Crystallization," *Progress in Polymer Science* 37, no. 12 (2012): 1657–1677, https://doi.org/10.1016/j.progpolymsci.2012.07.005.

20. C. B. Roth and J. R. Dutcher, "Glass Transition and Chain Mobility in Thin Polymer Films," *Journal of Electroanalytical Chemistry* 584, no. 1 (2005): 13–22, https://doi.org/10.1016/j.jelechem.2004.03.003.

21. E. Pregi, I. Romsics, R. Várdai, and B. Pukánszky, "Interactions, Structure and Properties of PLA/Lignin/PBAT Hybrid Blends," *Polymers* 15, no. 15 (2023): 3237, https://doi.org/10.3390/polym15153237.

22. K. Burns, I. D. V. Ingram, J. H. Potgieter, and S. Potgieter-Vermaak, "Synthesis and Performance Evaluation of Novel Soybean Oil-Based Plasticisers for Polyvinyl Chloride (PVC)," *Journal of Applied Polymer Science* 140, no. 45 (2023): e54656, https://doi.org/10.1002/app.54656.

23. W. Thimm, C. Friedrich, M. Marth, and J. Honerkamp, "An Analytical Relation Between Relaxation Time Spectrum and Molecular Weight Distribution," *Journal of Rheology* 43, no. 6 (1999): 1663–1672, https://doi.org/10.1122/1.551066.

24. H. Jang, J. Lee, M. K. Kwon, K. H. Seo, and K. S. Cho, "Analysis of PLA Blends Using Weighted Relaxation Spectrum," *Fibers and Polymers* 22, no. 2 (2021): 314–322, https://doi.org/10.1007/s12221-021-0121-z.

Supporting Information

Additional supporting information can be found online in the Supporting Information section.